JOURNAL OF MATERIALS SCIENCE 25 (1990) 3894–3900

# Influence of thermomechanical ageing on tensile properties of 2014 aluminium alloy

S. SINGH, D. B. GOEL
*Department of Metallurgical Engineering, University of Roorkee, Roorkee 247 667, India*

2014 aluminium alloy was subjected to various thermomechanical ageing (TMA) treatments which included partial peak ageing (25% and 50%), warm rolling (10% and 20%) and further ageing to peak hardness level at 160° C. The tensile tests reveal that TMA treatments cause a substantial improvement in tensile properties and thermal stability. The electron microscopic studies reveal that the TMA treatments affect substantially the ageing characteristics. The TMA Ib treatment yields the finest $\theta'$ needles having longitudinal dimensions of $\sim 40$ nm. The TMA treatments also lead to precipitate–dislocation networks of different densities. It is observed that TMA IIb treatment results in the densest precipitate–dislocation tangles of all the TMA treatments. As a result, a significant improvement in the tensile properties of 2014 aluminium alloy has been observed.

## 1. Introduction

Aluminium alloys are selected as materials of construction in many fields because of their low weight to volume ratio, ability to resist corrosion and capability of undergoing precipitation hardening treatment. These alloys can be safely used at low temperatures, but they start losing their strength when exposed to higher temperatures, primarily due to coarsening of the second-phase precipitated particles which are responsible for strengthening at lower temperatures. However, it should be possible to introduce a dislocation substructure which can withstand the effect of elevated temperatures without much loss in hardness and strength [1–6]. Thus, such a substructure should be a source of strength at elevated temperatures and responsible for controlling the coarsening of precipitate particles even at elevated temperatures.

By thermomechanical ageing (TMA) treatments, it is possible to develop a dislocation substructure which can control the coarsening of second-phase precipitate particles even after long exposures at elevated temperatures and such dislocation arrangement is responsible for improvement in the overall properties of aluminium alloys [6–10]. Although different cycles of TMA have been employed by different workers, the results obtained for tensile properties are positive. The reasons suggested for improvement in tensile properties are (i) introduction of a particular type of dislocation substructure [4–6, 9], (ii) optimization of precipitate size and shape [11, 12], and (iii) production of a homogeneous distribution of dislocations and precipitated particles [13].

## 2. Experimental procedure

The 2014 aluminium alloy of commercial purity was prepared, homogenized at 500° C and hot rolled at 425° C to the desired cross-sections. The final chemical composition of the alloy is given in Table I; iron was present as an impurity.

Tensile properties were measured after the following treatments: (i) as-quenched (solution treatment at 500° C, followed by quenching), (ii) peak-aged (artifical ageing at 160° C to peak hardness level), (iii) TMA Ia (25% preageing , 10% warm rolling and ageing to peak hardness value), (iv) TMA Ib (25% preageing, 20% warm rolling and ageing to peak hardness value), (v) TMA IIa (50% preageing, 10% warm rolling and ageing to peak hardness value). (vi) TMA IIb (50% preageing, 20% warm rolling and ageing to peak hardness value). In all the above treatments, warm rolling and ageing were carried out at 160° C. These treatments given to the alloy are shown schematically in Table II. Tensile tests were also carried out after 100 h exposure at 100, 150, 200 and 250° C after each of the above treatments. Tensile tests were conducted on 3.2 mm thick sheet specimens shown in Fig. 1 to suit the specific requirements of Monsanto tensometer type "W" and three specimens were tested after each treatment. The average values of ultimate tensile strength (UTS), yield strength (YS) (0.2% proof stress) and per cent elongation were calculated and recorded.

Structural changes during TMA treatments were studied with the help of a Metavert optical microscope and a Philips EM 400 transmission electron

TABLE I Nominal and actual compositions of 2014 aluminium alloy

| Element | Nominal range (wt %) | Actual composition of the alloy used in the present study (wt %) |
|---|---|---|
| Copper | 3.9–5.0 | 4.44 |
| Silicon | 0.5–1.2 | 0.85 |
| Manganese | 0.4–1.2 | 0.77 |
| Magnesium | 0.2–0.8 | 0.45 |
| Aluminium | Balance | Balance |


0022-2461/90 $03.00 + .12 

TABLE II Details of treatments employed in the present investigation

| Treatment designation | Schematic Representation | Details of Treatment |
|---|---|---|
| As Quenched (AQ) pct = % | 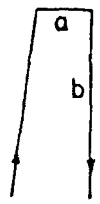  | a Solution treatment at 500°C for 1.50 hrs<br>b Quench in water |
| Peak aged (PA) pct = % | 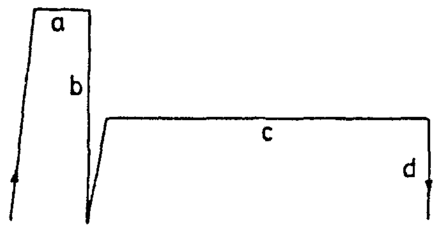  | a As above<br>b As above<br>c Peak ageing at 160°C<br>d Quench in water |
| TMA Ia pct = % | 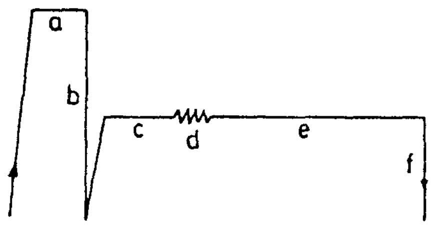  | a As above<br>b As above<br>c 25 pct preageing at 160°C (upto 73 VHN)<br>d 10 pct warm rolling at 160°C<br>e Final ageing at 160°C to peak value<br>f Quench in water |
| TMA Ib pct = % | 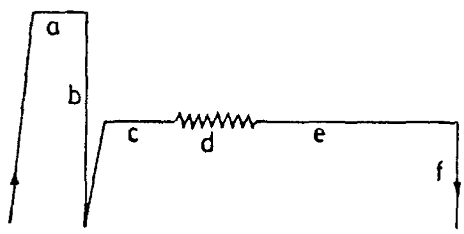  | a As above<br>b As above<br>c 25 pct preageing at 160°C<br>d 20 pct warm rolling at 160°C<br>e Final ageing at 160°C to peak value<br>f Quench in water |
| TMA IIa pct = % | 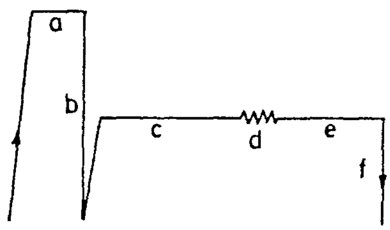  | a As above<br>b As above<br>c 50 pct preageing at 160°C (upto 87 VHN)<br>d 10 pct warm rolling at 160°C<br>e Final ageing at 160°C to peak value<br>f Quench in water |
| TMA IIb pct = % | 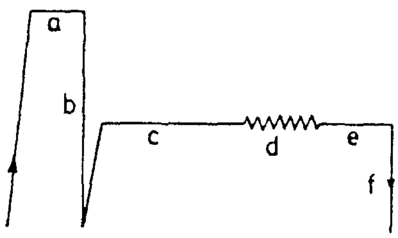  | a As above<br>b As above<br>c 50 pct preageing at 160°C<br>d 20 pct warm rolling at 160°C<br>e Final ageing at 160°C to peak value<br>f Quench in water |

microscope (TEM). For optical microscopic examination the specimens were polished by standard techniques and etched with HF. TEM studies were carried out on thin foil samples prepared by the window technique. Electro-thinning was carried out at 12 V and 70° C using the electrolyte (vol %) $H_3PO_4$ 62.00, $H_2O$ 24.00, $H_2SO_4$ 14.00 and $CrO_3$ 160 g $l^{-1}$.

## 3. Results

Fig. 2 shows a plot of the tensile properties resulting from TMA I and TMA II treatments against ageing time (h) on a log scale. It is seen that the strength rises to higher values in both the TMA teatments. It is also seen that the effect of TMA II type of treatment is more than that of TMA I treatment for both 10% and 20% deformations. In TMA I treatment, the UTS rises from 284 N $mm^{-2}$ to 321 and 333 N $mm^{-2}$ after 10% and 20% deformations, respectively, whereas in TMA II the UTS rises from 314 N $mm^{-2}$ to 341 and 371 N $mm^{-2}$ after 10% and 20% deformations,

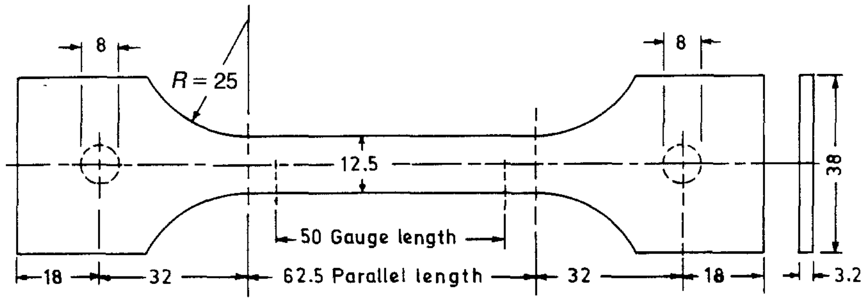


*Figure 1* Specimen for tensile testing. All dimensions in millimetres.

respectively. Thus increasing the deformation from 10% to 20% causes an increase of $29\,N\,mm^{-2}$ in the UTS by TMA II treatment, whereas in TMA I treatment the increase is only $13\,N\,mm^{-2}$.

The TMA IIb treatment raises the UTS from $375\,N\,mm^{-2}$ (achieved in the normal peak ageing) to a peak value of $432\,N\,mm^{-2}$ for a loss of elongation from 15% to 9.5%.

The peak values of tensile properties after 100 h exposure at 100, 150, 200 and 250° C are plotted in Figs 3 to 5. From Fig. 3 it can be seen that the UTS for peak-aged samples decreases from 375 to $178\,N\,mm^{-2}$ when exposed to 250° C for 100 h whereas in TMA IIb treated samples the UTS decreases from 432 to $346\,N\,mm^{-2}$ only. A similar effect has also been observed on yield strength as may be seen in Fig. 4. The elongation of peak-aged samples (Fig. 5) is observed to increase from 15% to 32%, whereas in the TMA IIb treated samples the elongation increases from 9.5% to 18%. Thus, it is seen that the TMA IIb treatment not only imparts maximum improvement but also provides maximum stability to tensile properties when exposed to higher working temperatures.

The TMA treatments substantially affect the ageing characteristics and the resultant microscopic structure of the alloy. The TMA Ib treatment yields the finest $\theta'$ needles having the longitudinal dimension of approximately 40 nm. The coarest-size $\theta'$ needles (~85 nm) are observed in peak-aged treatment (Fig. 6). The TMA treatments, besides affecting the ageing kinetics, also lead to dislocation–precipitate networks of different densities. In the present study it is observed that TMA IIb treatment results in the densest dislocation-precipitate tangles of all the thermomechanical treatments, whereas it is slightly less dense in TMA Ib treated alloy (Fig. 7). The treatments involving 10% deformation (TMA Ia and TMA IIa) yield microstructures depicting poor dislocation–precipitate interactions (Fig. 8).

In addition to $\theta'$ precipitate, two types of dispersoids [14] have also been observed, which have been identified as $Al_4CuMg_5Si_4$ and $Al_{12}(Fe, Mn)_3Si$. It has been observed, that there is a drastic reduction in the concentration of these dispersoids due to various TMA treatments.

## 4. Discussion

The effect of TMA treatments on various mechanical

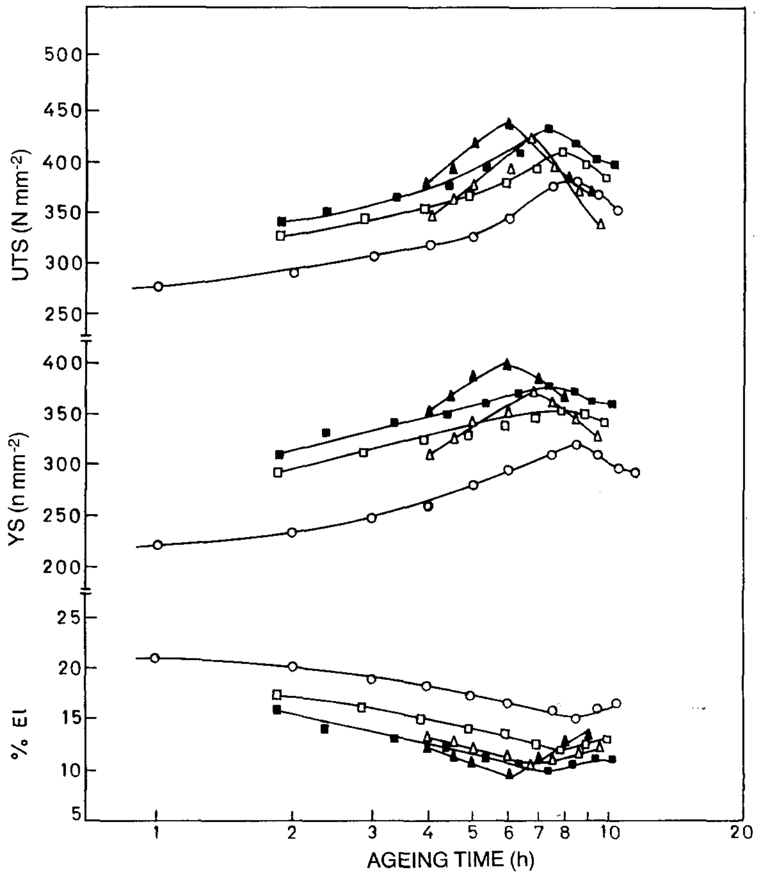


*Figure 2* Effect of thermomechanical ageing on tensile properties (○) Peak-aged, (□) TMA Ia, (■) TMA Ib, (△) TMA IIa, (▲) TMA IIb.

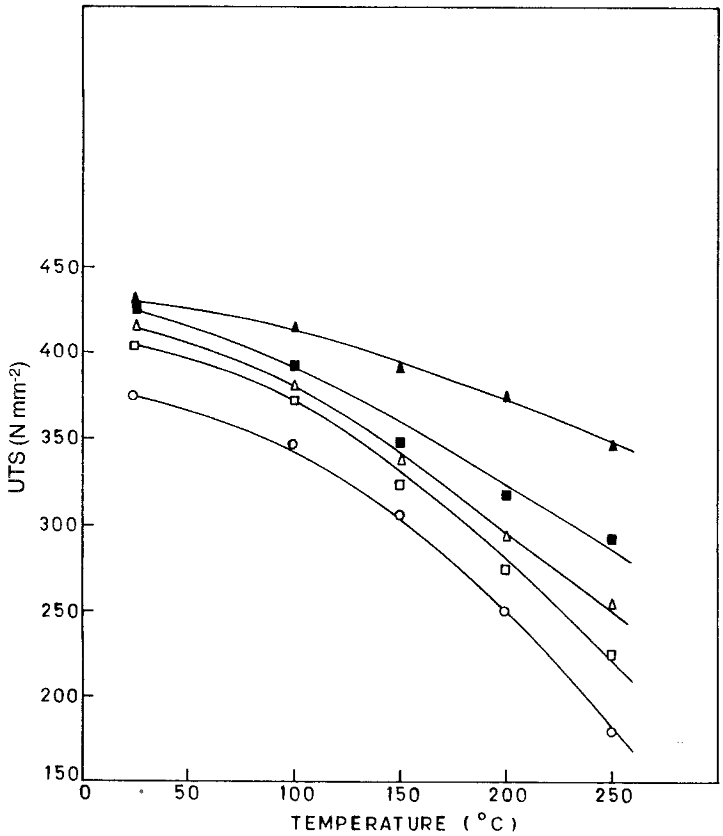


*Figure 3* Peak UTS values after different thermomechanical treatments and after 100 h exposure at different temperatures. For key, see Fig. 2.

properties has its origin in the structural characteristics of the alloy. Accordingly, the results of the investigation are explained in terms of size, shape and distribution of precipitates and the interaction with dislocations during the TMA treatments. All these parameters have been observed to be affected by (i) degree of preageing, which affects the solute concentration, (ii) degree of deformation, which affects the potential sites for precipitation of intermediate phases and enhances the diffusion rates, and (iii) final ageing treatment which governs the subsequent ageing steps and interaction of precipitates and dislocations.

The strengthening effects in the 2014 aluminium alloy after various TMA treatments may be considered to be due to (i) coherent precipitates $\theta''$, (ii) partially coherent $\theta'$ precipitates, and (iii) dislocation substructure. According to TEM observations, the GP II ($\theta''$) is formed only in the peak-ageing treatment

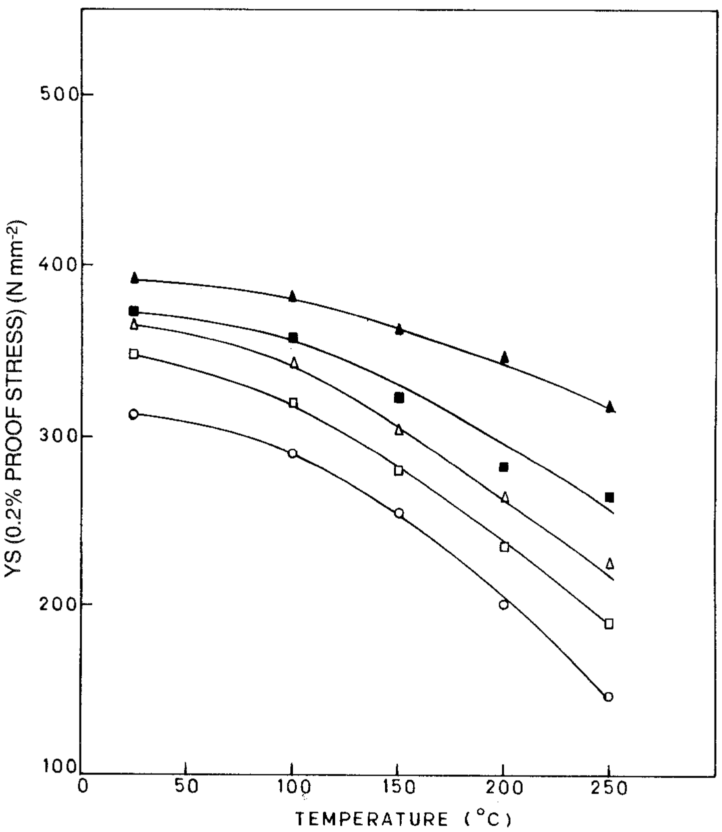


*Figure 4* Peak YS values after different thermomechanical treatments and after 100 h exposure at different temperatures. For key, see Fig. 2.

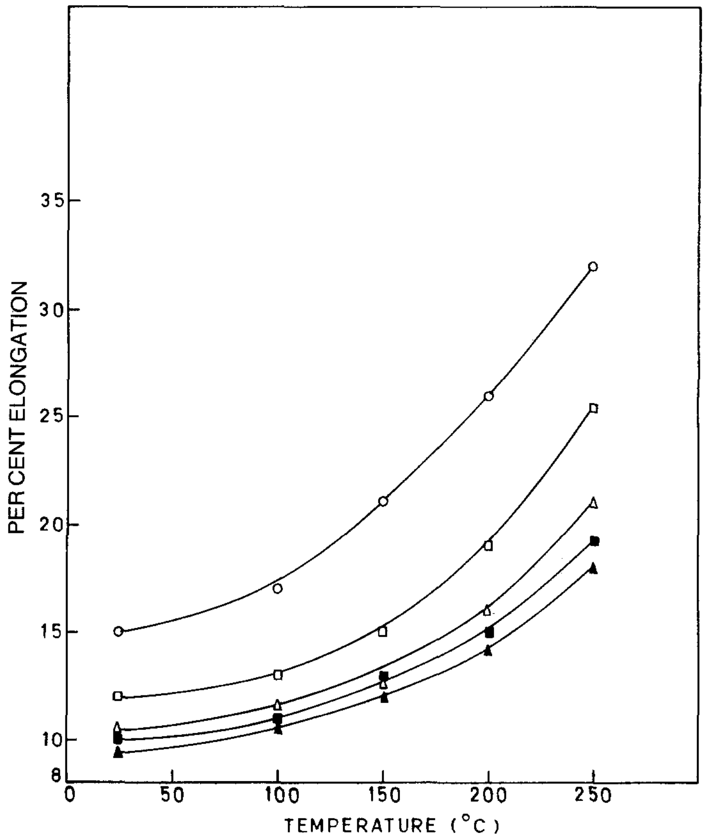


*Figure 5* Peak values of per cent elongation after different thermomechanical treatments and after 100h exposure at different temperatures. For key, see Fig. 2.

(Fig. 9). The increase in strength due to various thermomechanical treatments in the alloy under investigation may be attributed to the presence of $\theta'$ precipitates (Fig. 6), as has been observed by other investigators [15, 16]. The degree of strengthening resulting from the $\theta'$ precipitates depends on their size, mean interparticle spacing, volume fraction and their distribution in the matrix. All these factors are interrelated. The $\theta'$ particles may be cut by the dislocation at stress levels much above those required to move dislocations through the matrix phase. On the other hand, the $\theta'$ particles may also resist cutting and the dislocations may be forced to take a path around the obstacles, i.e. they can act as strong impenetrable particles through which the dislocations can move only by sharp changes in curvature of dislocations. It is believed that the first mechanism is operative only in the presence of GPI and GPII zones ($\theta''$), while in the presence of semi-coherent $\theta'$ particles the second mechanism appears to be operative. A dislocation may, in passing through the matrix, be arrested by the dispersion of $\theta'$ particles. The stress required to bulge round the particles is given by the expression

$$\tau = \frac{2Gb}{\lambda} \tag{1}$$

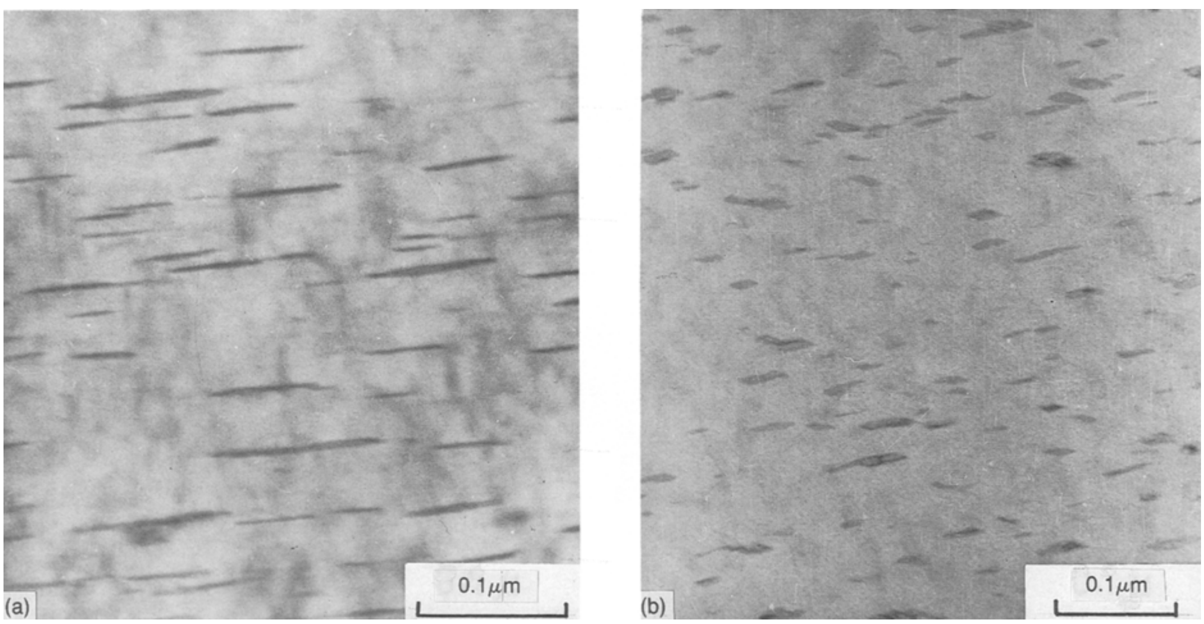


*Figure 6* Transmission electron micrographs of (a) peak-aged and (b) TMA Ib treated specimens.

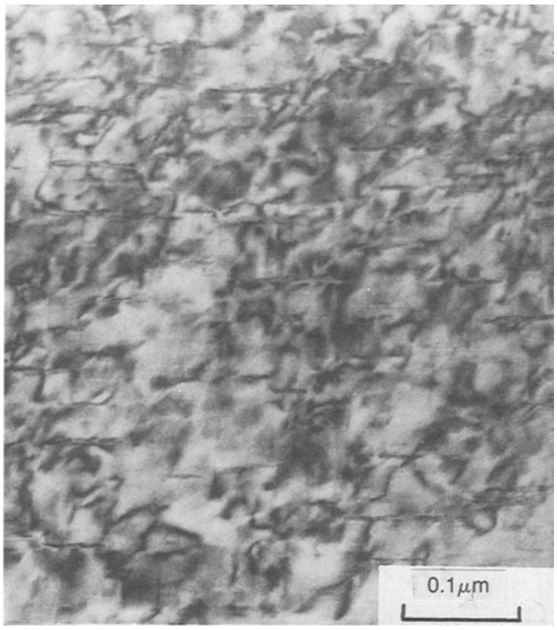


*Figure 7* Transmission electron micrograph of TMA IIb specimen showing dislocation–precipitate tangles.

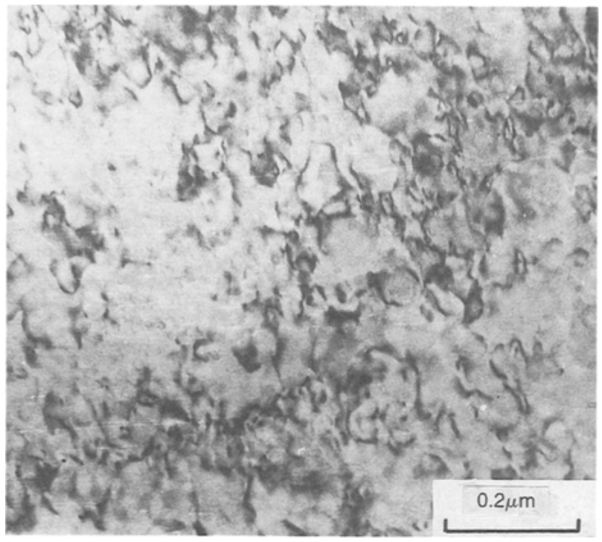


*Figure 8* Transmission electron micrograph of TMA Ia treated specimen showing dislocation–precipitate tangles.

where $G$ is the shear modulus, $\boldsymbol{b}$ the Burger's vector and $\lambda$ is interparticle spacing. This relation clearly shows that for a given volume fraction of $\theta'$, a higher stress, $\tau$, is required for a finer size of precipitate particles because this would result in a smaller interparticle spacing, $\lambda$. After bulging through between the particles, the dislocation line reforms, leaving a dislocation loop around the particles, effectively increasing its size and decreasing the spacing between nearby particles, so that an ever increasing stress is required to push successive dislocations through.

Besides the contribution of $\theta'$ particles, the dislocation substructure produced in the TMA treatments also plays a vital role in overall strengthening mechanism. The dislocation substructures produced during various TMA treatments consist of tangles of dislocations and dislocation cells as shown in Figs 7 and 8. The strengthening is caused by work-hardening effects produced between moving dislocations and the dislocation substructure. Staker and Holt [17] gave the following flow stress relationship

$$\tau \equiv \alpha G\boldsymbol{b}/\varrho^{1/2} \quad (2)$$

where $\alpha$ is a constant of the order 0.5, and $\varrho$ the dislocation density. According to Thompson [9] the flow stress is also related to the dislocation cell size

$$\tau = \alpha kG\boldsymbol{b}\boldsymbol{d}^{-1} \quad (3)$$

where $d$ is the dislocation cell diameter and $k$ is a constant for a given material. Higher flow stresses have been observed in smaller cells in accordance with this equation [6].

The existence of $Al_4CuMg_5Si_4$ and $Al_{12}$ (Fe, Mn)$_3$Si dispersoids contributes to the strengthening of the alloy only weakly and in contrast to the contribution of $\theta'$ and dislocation substructure, their effect on overall strengthening may be neglected. These dispersoids are very coarse in size [18] and can be seen easily under an optical microscope at low magnifications. The dispersoids are also mechanically weak particles and are observed to break at low stresses [18].

Because the nucleation of $\theta'$ particles is enhanced by the presence of dislocations, the strength will be high when fine $\theta'$ particles are formed in a dense dislocation cell structure.

The average diameters of $\theta'$ plates after various treatments have been estimated from TEM studies as follows: peak aged 85 nm; TMA Ia 65 nm; TMA Ib 40 nm; TMA IIa 75 nm; TMA IIb 60 nm. Bonfield and Datta [15] have established that the peak hardness in Al–Cu–Si–Mg alloy is associated with the presence of $\theta'$ precipitates of diameter up to 75 nm and an increase of diameter beyond 85 nm causes overageing effects. In the present study, the diameter of $\theta'$ particles in the peak-aged samples is approximately 85 nm. The hardness in the peak-aged conditions is associated with the presence of $\theta''$ and $\theta'$. In all the thermomechanically

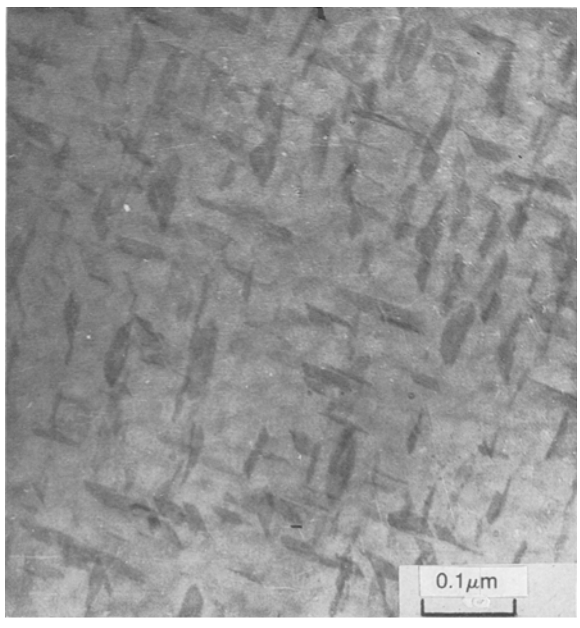


*Figure 9* Transmission electron micrograph showing the existence of predominently $\theta''$ platelets together with small amount of $\theta'$ in the peak-aged condition.

aged samples the peak hardness is associated only with $\theta'$ as no evidence of $\theta''$ is seen in these samples. Because the diameter of $\theta'$ precipitates in all the thermomechanically aged samples is less than 85 nm, it would appear that strengthening after various TMA treatments would be significantly governed by the nature of dislocation substructures. As revealed from TEM study, the dislocation density, $\varrho$, is maximum after TMA 11b treatment and decreases after various treatments in the order

$$\varrho_{\mathrm{TMA\,IIb}} > \varrho_{\mathrm{TMA\,Ib}} > \varrho_{\mathrm{TMA\,IIa}} > \varrho_{\mathrm{TMA\,Ia}} > \varrho_{\mathrm{peak\text{-}aged}}.$$

Thus strengthening after various thermomechanical treatments is also expected to be in this order. This explains the observations of YS (0.2% proof stress), UTS and percentage elongation after various treatments as given in Fig. 2. The TMA IIb treatment, therefore, provides maximum increase in YS and UTS. The peak-ageing treatment results in the poorest mechanical properties due to the coarsest $\theta'$ particle size and absence of dislocation–particle tangles. In the present study, the TMA IIb treatment raises the YS of 2014 aluminium alloy from 314 N mm$^{-2}$ (achieved in the normal peak-aged condition) to 392 N mm$^{-2}$ and UTS from 372 to 432 N mm$^{-2}$.

Attempts have also been made by several workers [4, 6, 9] to improve high-temperature performance of aluminium alloys by providing, through TMA treatments, a dislocation substructure which is stable at elevated temperatures. Such a substructure should be a source of strength at elevated temperatures. Figs 3 to 5 show the variation in UTS, YS and elongation, respectively, after an exposure of 100 h at various temperatures. It is seen that the stabilization of UTS and YS (0.2% proof stress) values is directly linked to the dislocation density in the dislocation substructures produced by different TMA treatments. Maximum stabilization in UTS and YS (0.2% proof stress) at elevated temperatures is observed in the alloy after TMA IIb treatment which produces the densest dislocation–particle tangles. The alloy after this treatment shows a 20% fall of UTS and YS (0.2% proof stress) values after 100 h exposure at 250° C, whereas in the alloy after peak ageing the drop in these properties is by 50%. Figs 3 to 5 show that exposure at elevated temperatures increases the elongation very steeply at the expense of small drops in the tensile strength.

The stabilisation of strength properties at elevated temperatures is considered to be due to the presence of fine $\theta'$ particles in the deformed structure, which inhibit recrystallization. TEM studies show practically no change in dislocation configuration of the TMA IIb treated alloy after 100 h exposure at 250° C. The interparticle spacing in all the thermomechanically treated samples ranges between 0.1 and 0.2 $\mu$m. This is in agreement with the observations of Doherty and Martin [19] and Pattanaik *et al.* [6] that recrystallization in Al–Cu alloys containing $\theta'$ is slowed down when the interparticle spacing is less than 1 $\mu$m.

In the light of the above discussion and on the basis of TEM observations it is concluded that the TMA IIb treatment not only provides maximum strengthening to 2014 aluminium alloy but also provides a dislocation–precipitate structure which is most effective in stabilizing the tensile strength at elevated temperatures.

## 5. Conclusions

The general strengthening of the alloy is attributed mainly to the existence of $\theta''$, $\theta'$ and dislocation–precipitate tangles. In the peak-aged material, the hardening occurs predominantly due to $\theta''$ platelets, whereas after TMA treatments the strengthening is mainly controlled by fine distribution of $\theta'$ precipitates and density of dislocations. The alloy after TMA IIb treatment exhibits maximum improvement in hardness and tensile properties. The TMA IIb treatment also provides a dislocation–precipitate structure which is most effective in stabilizing the tensile properties at elevated temperatures.

## References


1. N. RYUM, B. HAEGLAND and T. LINDVEIT, *Z. Metallkde* **58** (1967) 28.
2. N. RYUM, *Acta Metall.* **16** (1968) 327.
3. *Idem, ibid.* **17** (1969) 821.
4. H. A. LIPSITT and C. M. SARGENT, Proceedings of the International Conference on Strength of Metals and Alloys (ASM, 1970) p. 937.
5. H. A. LIPSITT, *Met. Trans* **2A** (1971) 1739.
6. S. PATTANAIK, V. SRINIVASAN and M. L. BHATIA, *Scripta Metall.* **6** (1972) 191.
7. H. J. RACK and R. W. KRENZER, *Met. Trans.* **8A** (1977) 335.
8. D. S. THOMPSON, S. A. LEVY and D. K. BENSON, Proceedings of the 3rd International Conference on Strength of Metals and Alloys, Cambridge, UK, Vol. 1 (1973) p. 119.
9. A. W. THOMPSON, *Met. Trans.* **8A** (1977) 833.
10. D. S. THOMPSON and S. A. LEVY, *Light Metal Age*, August (1977) 11.
11. E. DI RUSSO, M. CONSERVA, M. BURATTI and F. GATTO, *Mater. Sci. Engng* **14** (1974) 23.
12. J. WALDMAN, H. SULINSKI and H. MARKUS, *Met. Trans.* **5A** (1974) 573.
13. N. E. PATON and A. W. SOMMER, Proceedings of the 3rd International Conference on Strength of Metals and Alloys, Cambridge, UK Vol. 1 (1973) p. 101.
14. S. SINGH, PhD thesis, University of Roorkee (1985) p. 119.
15. W. BONFIELD and P. K. DATTA, *J. Mater. Sci.* **11** (1976) 1661.
16. R. H. VAN STONE, R. H. MERCHANT and J. R. LOW JR, ASTM STP 556 (American Society for Testing and Materials, Philadelphia, Pennsylvania, 1974) p. 93.
17. M. R. STAKER and D. L. HOLT, *Acta Metall.* **20** (1972) 569.
18. J. P. TANAKA, C. A. PAMPILLO and J. R. LOW JR, ASTM STP 463 (American Society for Testing and Materials, Philadelphia, Pennsylvania, 1970) 191.
19. R. P. DOHERTY and J. W. MARTIN, *J. Inst. Metals* **91** (1963) 332.



*Received 1 June 1988*
*and accepted 15 February 1989*